Asian Journal of Chemistry; *Vol. 38, No. 5 (2026), 1341-1352*

ASIAN JOURNAL OF CHEMISTRY

https://doi.org/10.14233/ajchem.2026.35782

Synthesis, Characterisation and *In silico* Evaluation of Novel 2-Methyl-Pyridin-3(2*H*)-one Derivatives

MANDHA SRUTHI, GUNNAM JAHNAVI, PICHEWAR SWASTHIKA, L. SAMPATH GOUD and K. SUDHA RANI*

Department of Pharmaceutical Chemistry, Gokaraju Rangaraju College of Pharmacy, Bachupally, Hyderabad-500118, India

*Corresponding author: E-mail: sudha.k377@gmail.com

Received: 1 March 2026 *Accepted*: 17 April 2026 *Published online*: 4 May 2026 AJC-22360

A novel series of 2-methyl-pyridin-3(2*H*)-one derivatives (**S1-S4**) was synthesised and evaluated for their physico-chemical, pharmacokinetic and biological potential using combined experimental and *in silico* approaches. The target compounds were obtained *via* a two-step synthetic route involving Claisen-Schmidt condensation to form chalcone intermediates, followed by alanine-mediated cyclisation to generate the pyridinone scaffold. The structural confirmation was achieved through elemental analysis, FTIR, ^{1}H NMR, ^{13}C NMR, and mass spectrometry. Computational studies revealed that all compounds possess favourable drug-like characteristics, complying with Lipinski's criteria and exhibiting suitable lipophilicity, polarity and molecular size. ADMET predictions suggested acceptable absorption, distribution, and excretion profiles, although metabolic studies highlighted cytochrome P450 inhibition, particularly CYP2C19 and CYP2C8, as a potential limitation. Toxicity assessment indicated variable safety profiles, with some compounds showing predicted risks of genotoxicity and hepatotoxicity. Molecular docking studies against microbial targets (1KZN and 6Q9N) demonstrated stable binding interactions, with compound **S2** exhibiting the most favourable interaction pattern and binding affinity. PASS analysis further supported the potential biological activity of the series, particularly for enzyme inhibition.

Keywords: 2-Methyl-pyridin-3(2*H*)-ones, Chalcones, Aldehydes, Alanine, *In silico* ADMET.

INTRODUCTION

Nitrogen-containing heterocycles are the most important in medicinal chemistry due to their presence in many bioactive molecules [1-3]. Among them, pyridine, a six-membered aromatic ring with one nitrogen atom, is a valuable pharmacophore with useful physico-chemical properties. Modification of the pyridine ring can enhance biological activity, making it an important scaffold for the synthesis of drugs [4,5].

Pyridine and its derivatives possess wide-ranging industrial and pharmaceutical significance [6,7]. They are employed as solvents and key intermediates in the synthesis of therapeutic agents such as sulphapyridine, antihistamines and antitubercular drugs including isoniazid, as well as in agrochemical production and rubber processing [8,9]. Owing to their importance, several synthetic strategies have been developed for the construction and functionalisation of pyridine-based heterocycles, including amination reactions [10-12], Chichibabin aromatic substitution [13], multicomponent transformations [14] and Kröhnke reactions [15,16]. The pyridine scaffold is an important structural motif in compounds exhibiting antibacterial [17,18], anticancer [19,20], anti-inflammatory [21], antitubercular [22], antidepressant, antiviral and analgesic activities [23]. In addition, pyridine derivatives are widely used as organocatalysts and versatile intermediates in organic synthesis [24].

Similarly, pyridinones are the important scaffolds in medicinal chemistry due to their ability to function as hydrogen bond donors and acceptors [25]. Their physico-chemical properties can be modulated through structural modification, enabling applications in fragment-based drug design and kinase hinge-binding motifs [25,26]. Pyridinones also act as bioisosteres for amides, pyridines, pyranones, pyrimidines, pyrazines and phenolic systems because of the relative positioning of the nitrogen and carbonyl group [27]. Chalcones are aromatic ketones that act as key intermediates in flavonoid biosynthesis and serve as valuable lead compounds in drug discovery [28]. Owing to their simple yet versatile structure, chalcones can be readily modified to optimize biological activity [29].

As members of the flavonoid family, they exhibit structural diversity and interact with multiple biological targets [30].

In view of the pharmacological importance of pyridine-based frameworks and the continuing demand for structurally diverse bioactive heterocycles, the present work focuses on the design and synthesis of a novel series of 2-methyl-pyridin-3(2*H*)-one derivatives. The target molecules were synthesised through strategically constructed chalcone intermediates followed by intramolecular cyclisation to generate the pyridone nucleus. Introduction of varied substituents was intended to modulate the electronic and steric environment of the scaffold, thereby enhancing its potential biological relevance. The newly synthesized derivatives were comprehensively characterised using standard spectroscopic techniques, establishing their structures and providing a basis for further biological and *in silico* evaluation.

EXPERIMENTAL

The chemicals and reagents used in the synthesis included *p*-nitrobenzaldehyde, *p*-aminoacetophenone, 4-bromobenzaldehyde, 4-hydroxyacetophenone, 2,4-dichlorobenzaldehyde, syringaldehyde, alanine and potassium hydroxide, procured from standard commercial suppliers and used without further purification.

Synthesis of 2-methyl-pyridin-3(2*H*)-one derivatives: Equimolar quantities (0.1 mol) of substituted acetophenone and aldehyde were reacted in ethanol (10 mL) in the presence of 40% aqueous KOH (10 drops) under trituration at room temperature for approximately 20 min to afford the corresponding chalcones, which were isolated and recrystallised. The obtained chalcones were subsequently treated with alanine (0.1 mol) under similar basic conditions to synthesise 2-methyl pyridin-3(2*H*)-one derivatives (**S_1-S_4**) (**Scheme-I**).

6-(4-Aminophenyl)-2-methyl-4-(4-nitrophenyl)pyridine-3(2*H*)-one (S_1): Yield: 79.2%; m.w.: 321.33; m.p.: 174-177 ºC; R_f: 0.8; Elemental analysis of $C_{18}H_{15}N_3O_3$: calcd. (found) % C: 67.28 (67.30) ; H: 4.71 (4.70); O: 13.08 (13.07); N, 14.93 (14.90); FTIR (KBr, ν_{max}, cm^{-1}): 3525 (NH_2 *str.*), 3090 (Ar–CH *str.*), 2996 (CH_3 *str.*), 1666 (C=O, pyridinone), 1596 (C=C/C=N), 1511 (NO_2 asymmetric), 1340 (NO_2 symmetric), 1286 (C–N *str.*), 994 (Ar–CH bending). ^{1}H NMR (400 MHz, $CDCl_3$, δ ppm): 2.28 (s, 3H, CH_3), 6.55-7.05 (m, 5H, Ar–H), 7.48 (s, 1H, H-5, pyridin-3-one), 7.62 (d, $J \approx 8.4$ Hz, 1H, Ar–H), 7.70 (d, $J \approx 8.4$ Hz, 1H, Ar–H), 9.80-10.20 (br s, 2H, NH_2), ~11.0 (br s, 1H, NH, pyridinone). ^{13}C NMR (400 MHz, $CDCl_3$, δ ppm): 116.5, 123.0, 124.8, 128.5, 129.2, (ArCH), 159.57 (C=C), 162.0 (C=O), 166.37 (C=N), 134.0, 139.5, 144.5, 151.0 (Cq), 163.5 (Cq, pyridone).

4-(2,4-Dichlorophenyl)-6-(4-hydroxyphenyl)-2-methyl-pyridin-3(2*H*)-one (S_2): Yield: 61.4%; m.w.: 346.21; m.p.: 154-158 ºC; R_f: 0.9; Elemental analysis of $C_{18}H_{13}Cl_2NO_2$: calcd. (found) % C, 62.43 (62.44); H, 3.78 (3.80); N, 4.05 (4.04); Cl, 20.47 (20.50); O, 9.24 (9.30); FTIR (KBr, ν_{max}, cm^{-1}) 3342 (OH), 1593 (-C=C/C=N), 3221 (Ar-CH *str.*), 754 (Ar-CH *bend.*), 1627 (C=O), 2885 (-CH_3), 1330 (CH bend, CH_3), 1170 (C-O), 1223 (C-N), 816 (C-Cl). ^{1}H NMR (400 MHz, $CDCl_3$, δ ppm): 12.10 (br s, 1H, NH), 9.85 (br s, 1H, OH), 7.92–7.35 (m, 7H, Ar–H), 6.78 (s, 1H, pyridin-3-one H), 2.29 (s, 3H, CH_3); ^{13}C NMR (400 MHz, $CDCl_3$, δ ppm): 167.8 (C=O), 156.2, 149.5 (pyridinone C), 145.8 (C–OH), 136.9, 134.4 (C–Cl), 131.8, 129.6, 128.9, 127.4, 125.6, 121.9 (Ar–C), 111.6 (pyridinone CH), 17.9 (CH_3).

6-(4-Aminophenyl)-4-(4-bromophenyl)-2-methylpyridin-3(2*H*)-one (S_3): Yield: 92.4.2%; m.w.: 357.25; m.p.: 165-175 ºC; R_f: 0.37; Elemental analysis of $C_{18}H_{17}BrN_2O$: calcd. (found) %: C, 60.52 (60.55); H, 4.80 (4.89); N, 7.84 (7.88);

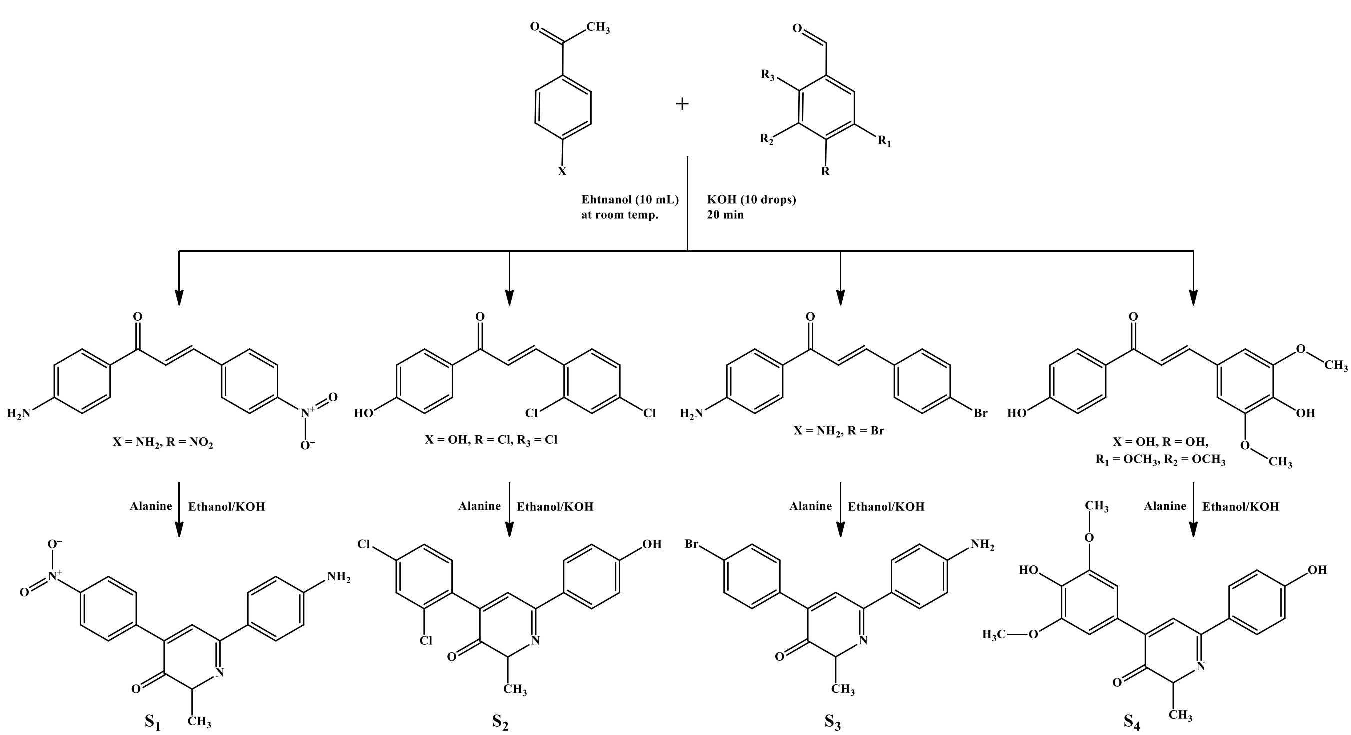

Scheme-I

Br, 22.37 (22.40); O, 4.48 (4.55); FTIR (KBr, ν_{max}, cm^{-1}): 3342 (NH_2), 1593 (Ar-C=C/C=N), 3220 (Ar-CH *str*.), 1171 (Ar-C-H *bend*.), 1650 (C=O), 2882 (CH_3), 1415 (CH *bend*., CH_3), 1628 (NH_2 *bend*.), 1223 (C-N *str*.), 818 (C-Br). ^1H NMR (400 MHz, $CDCl_3$, δ ppm): 11.95 (br s, 1H, NH, pyridin-3-one), 6.95-7.68 (m, 9H, Ar–H, bromo-phenyl + anilinyl), 6.62 (s, 1H, pyridin-3-one H), 5.12 (br s, 2H, NH_2), 2.27 (s, 3H, CH_3); ^{13}C NMR (400 MHz, $CDCl_3$, δ ppm): 168.2 (C=O), 156.8, 150.1 (pyridin-3-one C), 146.3 (C–NH_2), 137.5 (C–Br), 132.8, 130.6, 129.4, 128.1, 126.7, 123.9, 121.5 (Ar-C), 112.2 (pyridin-3-one CH), 18.1 (CH_3).

4-(4-Hydroxy-3,5-dimethoxyphenyl)-6-(4-hydroxyphenyl)-2-methylpyridin-3(2*H*)-one (S_4): Yield: 73.02%; m.f.: m.w.: 355.39; m.p.: 162-166 ºC, R_f: 0.34. Elemental analysis of $C_{20}H_{21}NO_5$: C, 67.59 (67.99); H, 5.96 (6.01); O, 22.51 (22.55); N, 3.94 (3.99); FTIR (KBr, ν_{max}, cm^{-1}): 3363 (br, O–H), 3105 (Ar–CH *str*.), 2912 (CH_3), 1690 (C=O), 1525 (C=C/C=N), 1431 (CH_3 *bend*.), 1418 (Ar–CH *bend*.), 1338 (C–N), 1252 (C–O), 1107 (C–O–C), 742 (Ar–H *bend*.). ^1H NMR (400 MHz, $CDCl_3$, δ ppm): 11.98 (br s, 1H, NH, pyridin-3-one), 9.82 (br s, 1H, Ar–OH), 9.45 (br s, 1H, Ar–OH), 7.48-6.65 (m, 7H, aromatic protons), 6.58 (s, 1H, H-5 of pyridin-3-one), 3.82 (s, 3H, OCH_3), 3.76 (s, 3H, OCH_3), 2.26 (s, 3H, CH_3); ^{13}C NMR (400 MHz, $CDCl_3$, δ ppm): 168.0 (C=O, pyridin-3-one), 157.6, 155.2, 151.0 (C–O and quaternary carbons of pyridinone and phenolic rings), 147.3 (C–OH), 139.2 (quaternary aromatic carbon, *ipso*-C), 131.8, 129.6, 127.9, 125.4, 121.6, 118.9 (aromatic CH carbons), 111.8 (C-5 of pyridin-3-one), 56.3, 55.8 (OCH_3), 18.0 (CH_3).

in silico Evaluation

The *in silico* assessment of the synthesised 2-methylpyridin-3(2*H*)-one derivatives (**S_1-S_4**) was performed using established computational platforms to evaluate drug-likeness, pharmacokinetic behaviour (ADMET), biological activity profiles and toxicity risks. All molecular structures were sketched and energy-minimised prior to analysis to ensure the optimal geometry for reliable predictions.

Molinspiration analysis: The physico-chemical descriptors and drug-likeness parameters were computed using the Molinspiration cheminformatics toolkit. Key properties, including partition coefficient (log P), topological polar surface area (TPSA), hydrogen bond donors (HBD), hydrogen bond acceptors (HBA) and molecular volume, were evaluated to determine compliance with Lipinski's rule of five and Veber's criteria for oral bioavailability. These parameters provide insight into membrane permeability, solubility and molecular flexibility [31,32].

OSIRIS property explorer: The toxicological risk assessment and drug-relevant properties were predicted using OSIRIS Property Explorer. The tool evaluates the structural fragments associated with mutagenicity, tumorigenicity, irritancy and reproductive toxicity, along with physico-chemical parameters such as cLogP, aqueous solubility (log S), drug-likeness and drug score, enabling early identification of potential safety liabilities [33].

PASS analysis: The biological activity prediction was carried out using PASS, which applies robust structure-activity relationship (SAR) models derived from large datasets of biologically active compounds. The probabilities of activity (Pa) and inactivity (Pi) were calculated, where higher Pa values indicate a greater likelihood of exhibiting specific pharmacological effects [34].

Molecular docking studies: The molecular docking simulations were conducted to investigate the ligand–target interactions with selected microbial proteins (PDB ids 1KZN and 6Q9N), retrieved from the Protein Data Bank. Protein structures were prepared by removal of water molecules, addition of hydrogen atoms and assignment of appropriate charges. Docking was performed using standard algorithms and binding conformations were analysed based on binding energy and interaction profiles, including hydrogen bonds, electrostatic interactions, π-π stacking and hydrophobic contacts. These interactions were used to rationalise binding affinity and stability within the active site [35,36].

ADMET prediction: Pharmacokinetic properties were predicted using SwissADME, pkCSM and admetSAR platforms. Absorption parameters such as Caco-2 permeability, MDCK permeability and P-glycoprotein interaction were assessed to estimate intestinal uptake and efflux liability. The distribution properties including blood–brain barrier (BBB) permeability, plasma protein binding and volume of distribution were analysed. Metabolic stability and drug–drug interaction potential were evaluated based on cytochrome P450 (CYP450) enzyme inhibition and substrate specificity. Excretion parameters such as total clearance and half-life were also predicted to understand the systemic elimination profiles [37-39].

BOILED-Egg and bioavailability radar: The graphical models including the BOILED-Egg and bioavailability radar, were generated using SwissADME to visualise passive gastrointestinal absorption, BBB penetration, lipophilicity, polarity, size, flexibility and solubility. These models provide an integrated representation of drug-likeness and pharmacokinetic suitability [37].

Toxicity and toxicophore analysis: Toxicity prediction was carried out using ProTox-II and Tox21 pathway-based models to assess endpoints such as hepatotoxicity, cardiotoxicity (hERG inhibition), mutagenicity, carcinogenicity and cytotoxicity. Toxicophore screening and rule-based filters were applied to identify structural alerts associated with adverse effects. In addition, the pathway-based analysis enabled the identification of potential interactions with nuclear receptor and stress-response signalling pathways, providing mechanistic insight into predicted toxicological outcomes [40,41].

RESULTS AND DISCUSSION

A series of 2-methyl-pyridin-3(2*H*)-one derivatives (**S_1-S_4**) were synthesised through a two-step synthetic sequence. In the first step, substituted acetophenones and aromatic aldehydes underwent base-mediated Claisen–Schmidt condensation in ethanolic KOH to generate the corresponding chalcone intermediates. In the second step, these intermediates were reacted with alanine under alkaline conditions, where alanine served as a nitrogen donor. The reaction proceeds *via* Michael conjugate addition to the α,β-unsaturated system, followed by intramolecular ring closure and dehydration, yielding the pyridinone framework. The method afforded the target compounds in moderate to high yields (61-92%), demonstrating good synthetic efficiency. Furthermore, elemental analysis values were consistent with theoretical compositions, indicating good purity of the synthesised compounds.

The FTIR spectra of all compounds (**S_1-S_4**) displayed a prominent carbonyl absorption band for the pyridinone moiety in the region ~1690-1627 cm^{-1}, indicating successful ring formation. The absence of characteristic chalcone bands and the presence of functional group-specific signals such as $-NH_2$ (**S_1**, **S_3**), –OH (**S_2**, **S_4**) and halogen substituents further supported the transformation. ^{1}H NMR spectra showed a distinct singlet for the C-2 methyl group at δ ~2.2-2.3 ppm and a characteristic signal for the pyridinone proton (H-5) around δ ~6.5-7.5 ppm. Exchangeable protons corresponding to –NH and –OH groups appeared as broad signals in the downfield region (δ ~9.5-12 ppm). The aromatic protons were also observed within the expected range (δ ~6.5-8.0 ppm). ^{13}C NMR spectra exhibited signals corresponding to the carbonyl carbon (δ ~167-168 ppm), along with resonances for aromatic and heterocyclic carbons, confirming the formation of the conjugated pyridinone system.

In silico predictions

Molinspiration: The physico-chemical properties of the **S_1-S_4** compounds were evaluated using Molinspiration to assess their drug-likeness and oral bioavailability. All compounds complied with Lipinski's rule of five. The log P values ranged from 1.94 to 3.87, indicating moderate lipophilicity within the acceptable limit (<5). PSA values (49.66-101.28 Å^2) were below the recommended threshold (<140 Å^2), suggesting favourable membrane permeability. HBA (3-6) and HBD (1-2) values were within acceptable limits (HBA ≤10, HBD ≤5), supporting good hydrogen bonding potential and permeability. The molecular volumes ranged from 276.83 to 314.79 Å^3, indicating suitable size for receptor binding and membrane diffusion (Table-1). Based on these results, all compounds exhibited favourable drug-like properties, with compound **S_2** showed relatively most promising candidate due to its optimal lipophilicity and low PSA, suggesting good oral bioavailability and therapeutic potential.

OSIRIS property explorer: The **S_1-S_4** compounds were evaluated using OSIRIS property explorer to predict toxicity risks and key drug-related parameters. Toxicity prediction indicated that compound **S_1** showed risks of mutagenicity, tumorigenicity and reproductive toxicity, while compound **S_4** exhibited reproductive toxicity risk. In contrast, compounds **S_2** and **S_3** showed no predicted toxicity risks, suggesting better safety profiles. All compounds had molecular weights below 400 Da and acceptable cLogP values (1.66–3.80). Predicted solubility was satisfactory, with compound **S_4** showing relatively higher solubility. Drug-likeness and drug score analysis identified compound **S_2** as the most promising candidate (DL = 4.74; DS = 0.82), followed by compound **S_3** (DS = 0.78). Compound **S_4** showed moderate potential, whereas compound **S_1** had the lowest drug score (0.26) due to predicted toxicity and lower solubility (Table-2).

PASS analysis: PASS analysis was performed to predict the biological activities of compounds **S_1-S_4** based on probability of activity (Pa) and inactivity (Pi). All compounds exhibited Pa values (0.713-0.875) significantly higher than Pi (0.005–0.01), indicating a strong likelihood of biological activity. Compound **S_2** showed the highest Pa value (0.875), suggesting strong therapeutic potential, particularly in enzyme inhibition and anti-seborrheic activity. Compound **S_4** also demonstrated high activity (Pa = 0.820) with predicted enzyme inhibition and possible CYP-related interactions. Compound **S_1** (Pa = 0.764) exhibited notable enzyme inhibitory potential, while compound **S_3** (Pa = 0.713) showed moderate predicted activity including effects on neuromuscular and cell regulatory targets (Table-3).

CB docking: The selected protein targets, 1KZN and 6Q9N, are associated with microbial survival and pathogenic mechanisms and were chosen to evaluate the antimicrobial

TABLE-1
DETAILS OF MOLINSPIRATION-BASED MOLECULAR DESCRIPTORS OF SYNTHESISED COMPOUNDS (**S_1-S_4**)

Compound	IUPAC name	Log P	Polar surface area	H-bond acceptor	H-bond donor	Volume
S_1	6-(4-Aminophenyl)-2-methyl-4-(4-nitrophenyl)pyridine-3-(2*H*)-one	2.10	101.28	6	2	282.28
S_2	4-(2,4-dichlorophenyl)-6-(4-hydroxyphenyl)-2-methylpyridin-3(2*H*)-one	3.87	49.66	3	1	282.75
S_3	6-(4-aminophenyl)-4-(4-bromophenyl)-2-methylpyridine-3-(2*H*)-one	2.94	55.46	3	2	276.83
S_4	4-(4-hydroxy-3,5-dimethoxyphenyl)-6-(4-hydroxyphenyl)-2-methylpyridine-3-(2*H*)-one	1.94	88.36	6	2	314.79

TABLE-2
DETAILS OF OSIRIS PREDICTED TOXICITY RISKS OF SYNTHESISED COMPOUNDS (**S_1-S_4**)

Compound	Toxicity risks				Molecular properties calculation				
	MUT	TUMO	IRRI	REP	M.W	CLP	LogS	DL	DS
S_1					323.35	1.66	-4.48	2.76	0.26
S_2					346.21	3.80	-4.95	4.74	0.82
S_3					355.23	2.99	-4.68	1.36	0.78
S_4					353.37	2.11	-3.21	4.59	0.54

MUT: Mutagenic; TUMO: Tumorigenic; IRRI: Irritant; REP: Reproductive effective; CLP: CLogP; Log s: Solubility mol/L; DL: Drug-likeness; DS: Drug-score. MW: Molecular weight.

TABLE-3
PASS-PREDICTED BIOLOGICAL ACTIVITY PROFILES AND PROBABLE PHARMACOLOGICAL TARGETS OF SYNTHESISED COMPOUNDS (**S_1-S_4**)

Compound	P_a	P_i	Other predicted biological activities
S_1	0.764	0.005	Aryl-acylamidase inhibitors (0.764) Ubiquinol-cytochrome-c reductase inhibitor (0.755) Lysase inhibitors (0.727) Chymosin inhibitors (0.679)
S_2	0.875	0.006	Anti-seborrheic (0.875) Chlordecone reductase inhibitors (0.789) Ubiquinol-cytochrome-c reductase inhibitors (0.699) Aryl-acylamidase inhibitors (0.552)
S_3	0.713	0.007	Centromere associated protein inhibitors (0.713) Aspulvinone dimethylallyltransferase inhibitor (0.596) Acetylcholine neuromuscular blocking agents (0.582) Endothelial growth factor antagonist (0.471)
S_4	0.820	0.01	Aspulvinone dimethylallyltransferase inhibitor (0.809) Chlordecone reductase inhibitors (0.776) CYP2C12 substrate (0.765) Anti-seborrheic (0.745)

potential of the synthesised pyridin-3(2*H*)-one derivatives. Targeting such proteins is important for inhibiting microbial growth and function, thereby supporting the biological relevance of the docking study. All synthesised compounds (**S_1-S_4**) showed stable binding within the active sites of both target proteins (1KZN and 6Q9N), supported by hydrogen bonding, electrostatic forces, π-interactions and hydrophobic contacts. In the case of 1KZN, most compounds formed a key hydrogen bond with Asn46 and exhibited important π-interactions with Glu50 and Arg76, which contributed significantly to binding stability. The surrounding hydrophobic residues such as Val, Ile, Ala and Pro further strengthened ligand accommodation within the binding pocket. Among the series, compound **S_2** demonstrated the most favourable interaction profile, with strong hydrogen bonding and multiple π-anion and π-cation interactions, indicating enhanced binding affinity (docking score -8.7). For 6Q9N, all compounds formed stable complexes through conventional H-bonds along with hydrophobic and π-mediated interactions. Compound **S_2** again displayed stronger and more diverse interactions, including hydrogen bonding and multiple hydrophobic contacts, suggesting better stabilisation within the active site (docking score -8.8). The remaining compounds also showed satisfactory binding modes with balanced polar and nonpolar interactions. These interaction patterns indicate that the compounds are capable of effectively occupying the active site and may interfere with essential microbial processes, thereby supporting their potential anti-microbial activity (Fig. 1). From the docking results, it is concluded that all compounds possess good binding potential, with compound **S_2** appears as the most leading molecule due to its stronger and more consistent interactions across both targets.

Physico-chemical properties: The predicted physico-chemical properties of compounds **S_1-S_4** (Table-4) indicate favourable drug-like characteristics. All compounds possess acceptable molecular weights (321.11-354.04 g/mol) and suitable structural compactness. Hydrogen-bond acceptors (3-6) and donors (1-2) were within recommended limits. The presence of three rings, limited rotatable bonds (2-4) and low flexibility indices suggests relatively rigid molecular frameworks. All the compounds were found to lack stereocenter, consistent with their planar structures. TPSA values (49.66-98.59 Å^2) and moderate lipophilicity (logP 1.90-3.02; logD 2.26-3.15) support good membrane permeability. Although aqueous solubility was predicted to be low (logS -3.52 to -4.53), other parameters, including pK_a values and thermal stability, were within acceptable ranges.

Absorption: *In silico* absorption analysis suggested that compounds **S_1-S_4** possess generally acceptable oral absorption profiles. The Caco-2 and MDCK permeability values for all compounds fell within or near the optimal range, indicating moderate intestinal and membrane permeability. Although PAMPA results classified all compounds as low passively permeable, the favourable cellular permeability models suggest that absorption may not rely solely on passive diffusion. All compounds demonstrated low P-glycoprotein substrate liability, reducing the risk of efflux-mediated absorption loss. Compounds **S_3** and **S_4** showed higher probabilities of P-gp inhibition, which may further support intestinal uptake. Human intestinal absorption (≥30%) was predicted to be favourable for compounds **S_1-S_3**, while compound **S_4** showed acceptable absorption despite borderline permeability. The oral bioavailability predictions indicated a low risk of poor exposure at lower thresholds (F20% and F30%), although compound **S_4** may exhibit reduced bioavailability at higher systemic levels (F50%) (Table-5).

Distribution: The predicted distribution parameters of compounds **S_1-S_4** indicated generally acceptable distribution characteristics with distinct compound-specific trends. Compound **S_1** displayed moderate plasma protein binding (<90%), an adequate unbound fraction and low blood–brain barrier (BBB) permeability, supporting favourable systemic exposure for non-CNS targets. In contrast, compounds **S_2** and **S_3** showed high plasma protein binding with reduced free drug fractions, which may limit pharmacological availability, compound **S_3** additionally exhibited pronounced BBB penetration, suggesting potential central nervous system exposure. All compounds showed volumes of distribution within or

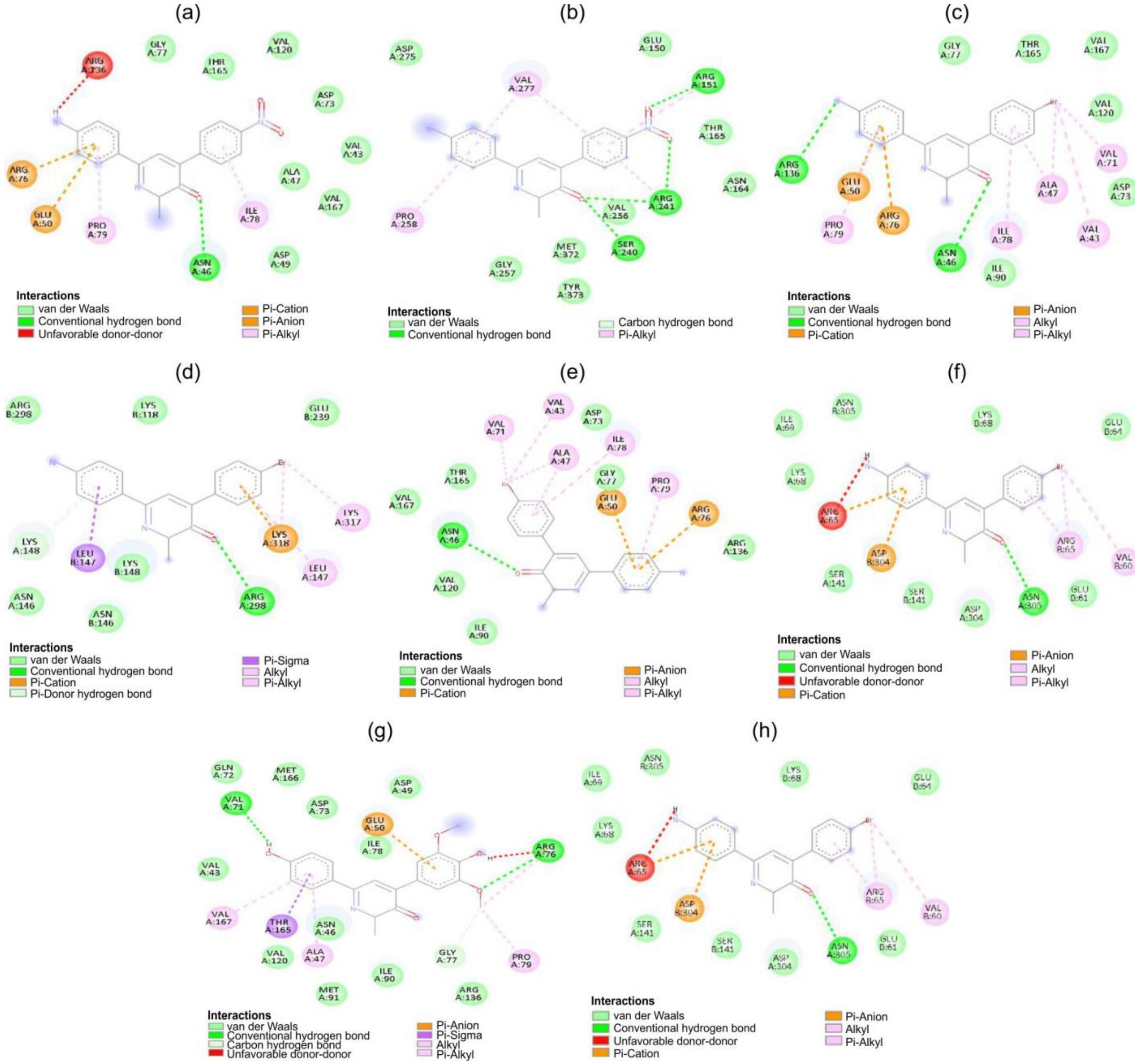

Fig. 1. 2D Molecular docking interactions of synthesised pyridin-3(2*H*)-one derivatives (**S_1-S_4**) with microbial target proteins 1KZN and 6Q9N

near the optimal range, indicating controlled tissue distribution without excessive accumulation, although compound **S_4** demonstrated limited extravascular distribution. Transporter interaction analysis revealed low inhibition potential toward OATP1B1/1B3 and BCRP for most compounds; however, MRP1 inhibition was consistently predicted across the series. Notably, compound **S_4** showed strong inhibition of multiple transporters, indicating an increased risk of transporter-mediated drug-drug interactions (Table-6).

Metabolism: *In silico* metabolism predictions revealed distinct cytochrome P450 (CYP) interaction profiles across compounds **S_1-S_4**. **S_1** exhibited favourable metabolic stability with low predicted human liver microsomal (HLM) instability and limited involvement of CYP1A2, CYP2C9 and CYP2D6; however, strong inhibition of CYP2C19, CYP2B6 and CYP2C8 was observed, indicating a potential risk of metabolic drug–drug interactions. Compounds **S_2** and **S_4** showed extensive CYP involvement, with high probabilities of both inhibition and substrate behaviour toward major isoforms, particularly CYP1A2, CYP2C19 and CYP3A4, suggesting significant hepatic metabolism accompanied by an elevated interaction liability. These trends were supported by moderate to high predicted HLM instability, especially for compound **S_4**, while compound **S_3** demonstrated high metabolic stability with minimal substrate behaviour across most CYP isoforms, although strong inhibitory effects toward CYP2C19, CYP2C9, CYP2B6 and CYP2C8 were predicted (Table-7). These results suggest that all the synthesised compounds demonstrate generally acceptable metabolic stability; however, significant CYP inhibition, particularly of CYP2C19 and CYP2C8, represents a key liability that requires further structural optimisation and experimental validation.

TABLE-4
DETAILS OF PHYSICO-CHEMICAL PROPERTIES OF SYNTHESISED COMPOUNDS (S_1-S_4) AND REFERENCE DRUG (CICLOPIROX)

Parameters	S_1	S_2	S_3	S_4	Ciclopirox
Molecular weight	321.11	345.03	354.04	353.13	207.13
Volume	327.211	329.486	320.554	360.027	219.663
Density	0.981	1.047	1.104	0.981	0.943
Nha	6.0	3.0	3.0	6.0	3.0
Nhd	2.0	1.0	2.0	2.0	1.0
NRot	3.0	2.0	2.0	4.0	1.0
NRing	3.0	3.0	3.0	3.0	2.0
MaxRing	6.0	6.0	6.0	6.0	6.0
NHet	6.0	5.0	4.0	6.0	3.0
FChar	0.0	1.0	0.0	0.0	0.0
NRig	20.0	19.0	19.0	19.0	13.0
Flexibility	0.15	0.105	0.105	0.211	0.077
Stereo centres	0.0	0.0	0.0	0.0	0.0
TPSA	98.59	49.66	55.45	88.35	42.23
LogS	-3.861	-4.528	-4.431	-3.523	-3.446
LogP	1.989	2.893	3.022	1.904	2.258
logD7.4	2.52	2.726	3.146	2.258	2.135
Pka (acid)	9.856	7.915	9.008	8.253	6.632
Pka (base)	3.939	3.878	4.121	6.177	3.068
Melting point	210.13	180.177	169.157	186.633	152.814
Boiling point	361.23	326.658	335.182	315.282	298.305

TABLE-5
DETAILS OF ABSORPTION AND PERMEABILITY-RELATED DRUGLIKENESS PARAMETERS OF SYNTHESISED COMPOUNDS (**S_1-S_4**) AND REFERENCE DRUG (CICLOPIROX)

Parameter	S_1	S_2	S_3	S_4	Ciclopirox
Caco-2 permeability	-4.703	-4.732	-4.644	-5.151	-4.784
MDCK permeability	-4.527	-4.817	-4.621	-4.835	-4.59
PAMPA	0.785	0.244	0.218	0.212	0.044
Pgp inhibitor	0.121	0.574	0.735	0.772	0.326
Pgp substrate	0.106	0.096	0.049	0.253	0.005
HIA	0.0	0.0	0.0	0.0	0.006

TABLE-6
DETAILS OF DISTRIBUTION AND TRANSPORTER INHIBITORY PROFILES OF SYNTHESISED COMPOUNDS (**S_1-S_4**) AND REFERENCE DRUG (CICLOPIROX)

Parameter	S_1	S_2	S_3	S_4	Ciclopirox
PPB	82.738	97.587	95.23	90.734	96.991
VDss	0.332	0.169	0.474	-0.298	-0.296
BBB	0.188	0.541	0.994	0.223	0.059
Fu	17.139	1.84	3.482	10.6	2.626
OATP1B1 inhibitor	0.039	0.286	0.383	0.889	0.977
OATP1B3 inhibitor	0.142	0.155	0.446	0.726	0.982
BCRP inhibitor	0.0	0.002	0.0	0.176	0.047
MRP1 inhibitor	0.992	0.941	0.608	0.976	0.984

Excretion: *In silico* excretion analysis indicated low to moderate plasma clearance across the series, with predicted clearance values ranging from 2.45 to 6.20 mL/min/kg. Compounds **S_1** and **S_3** exhibited low plasma clearance (<5 mL/min/kg), suggesting slower systemic elimination and prolonged exposure, whereas **S_2** and **S_4** showed moderate clearance (5-15 mL/min/kg), indicative of balanced elimination kinetics. Despite these differences, all compounds were predicted to have short elimination half-lives ($T_{1/2} \approx 1.1$-2.0 h), classifying them as short half-life drugs (Table-8). Thus, the excretion profiles suggest manageable systemic persistence with no evidence of excessive accumulation. However, the consistently short half-lives across the series indicate that frequent dosing or formulation strategies may be required to sustain therapeutic plasma concentrations during *in vivo* application.

Medicinal chemistry: All the synthesised compounds **S_1-S_4** demonstrated favourable medicinal chemistry profiles with moderate to high drug-likeness (QED = 0.533-0.898) and good synthetic feasibility (GASA = 1.0; synthetic accessibility = 3.0). All compounds showed high MCE-18 values (>52), supporting their potential for medicinal chemistry optimisation, although low Fsp^3 values indicated predominantly planar

TABLE-7
DETAILS OF CYTOCHROME P450-MEDIATED METABOLIC PROPERTIES AND HUMAN LIVER MICROSOMAL (HLM) STABILITY PROFILES OF SYNTHESISED COMPOUNDS (**S_1-S_4**) AND REFERENCE DRUG (CICLOPIROX)

Parameter	**S_1**	**S_2**	**S_3**	**S_4**	Ciclopirox
CYP1A2 inhibitor	0.125	0.959	0.536	0.941	0.459
CYP1A2 substrate	0.154	0.959	0.002	0.811	0.386
CYP2C19 inhibitor	0.923	0.999	0.999	1.0	0.0
CYP2C19 substrate	0.0	0.513	0.0	1.0	0.001
CYP2C9 inhibitor	0.34	0.996	0.998	0.664	0.002
CYP2C9 substrate	0.001	0.19	0.003	0.309	0.003
CYP2D6 inhibitor	0.0	0.0	0.0	0.0	0.0
CYP2D6 substrate	0.0	0.0	0.0	0.0	0.003
CYP3A4 inhibitor	0.517	0.686	0.28	0.925	0.001
CYP3A4 substrate	0.355	0.963	0.027	0.989	0.286
CYP2B6 inhibitor	0.822	0.145	0.827	0.002	0.056
CYP2B6 substrate	0.0	0.004	0.0	0.0	0.0
CYP2C8 inhibitor	1.0	0.991	1.0	0.992	0.316
HLM Stability	0.053	0.516	0.007	0.629	0.085

TABLE-8
DETAILS OF EXCRETION PARAMETERS OF SYNTHESISED COMPOUNDS (**S_1-S_4**) AND REFERENCE DRUG (CICLOPIROX)

Parameter	**S_1**	**S_2**	**S_3**	**S_4**	Ciclopirox
CL_{plasma}	2.989	5.69	2.446	6.201	8.155
$T_{1/2}$	1.61	1.083	1.735	1.953	1.188

architectures. The compounds largely complied with Lipinski, Pfizer, GSK and Golden Triangle rules, with only a single Pfizer violation observed for compound **S_3**. PAINS and BMS alerts were absent across the series, while ALARM NMR alerts suggested possible thiol reactivity. Remarkably, three compounds **S_1-S_3** exhibited high colloidal aggregation and fLuc inhibition probabilities indicating potential assay interference, whereas compound **S_4** showed reduced aggregation risk and a more balanced profile (Table-9). Thus, compound **S_4** demonstrated a more balanced medicinal chemistry profile with lower aggregation and reduced promiscuity risk, while compound **S_2** remained the most promising lead compound based on the studied biological and pharmacokinetic results.

Toxicophore rules: Toxicophore-based screening of compounds **S_1-S_4** revealed no alerts for acute oral toxicity or non-genotoxic carcinogenicity across the series, indicating a generally favourable primary safety profile. However, variable genotoxic carcinogenicity alerts were observed (1-11 alerts), suggesting the presence of structural motifs associated with potential mutagenic liability, particularly pronounced in

TABLE-9
DETAILS OF MEDICINAL CHEMISTRY DESCRIPTORS, DRUG-LIKENESS FILTERS AND STRUCTURAL ALERT PROFILES OF SYNTHESISED COMPOUNDS (**S_1-S_4**) AND STANDARD DRUG (CICLOPIROX)

Parameter	**S_1**	**S_2**	**S_3**	**S_4**	Ciclopirox
QED	0.533	0.898	0.832	0.882	0.719
SAscore	3.0	3.0	3.0	3.0	2.0
GASA	1.0	1.0	1.0	1.0	0.0
Fsp^3	0.111	0.111	0.111	0.2	0.583
MCE-18	55.8	55.8	52.7	58.583	28.947
NPscore	-0.247	0.198	0.065	0.655	0.301
Lipinski rule	Accepted	Accepted	Accepted	Accepted	Accepted
Pfizer rule	Accepted	Accepted	Rejected	Accepted	Accepted
GSK rule	Accepted	Accepted	Accepted	Accepted	Accepted
Golden Triangle	Accepted	Accepted	Accepted	Accepted	Accepted
PAINS	0	0	0	0	0
Alarm_NMR rule	3	2	3	3	0
BMS rule	0	1	0	0	0
Chelating rule	0	0	0	1	1
Colloidal aggregators	0.999	0.993	0.997	0.116	0.057
FLuc inhibitors	0.481	0.734	0.869	0.906	0.102
Blue fluorescence	0.139	0.395	0.376	0.499	0.043
Green fluorescence	0.904	0.494	0.979	0.693	0.488
Reactive compounds	0.147	0.186	0.104	0.034	0.166
Promiscuous compounds	0.123	0.12	0.039	0.147	0.042

compounds $\mathbf{S_1}$ and $\mathbf{S_3}$. Skin sensitisation alerts (2-6) were consistently detected, indicating a moderate to high risk of dermal irritation. Environmental assessments identified multiple aquatic toxicity (2-3) and non-biodegradability (1-3) alerts, suggesting moderate environmental persistence and aquatic hazard potential. No SureChEMBL alerts were observed, supporting acceptable medicinal chemistry characteristics, while limited FAF-Drug $\mathbf{S_4}$ alerts (2-4) indicated the presence of known toxic substructures (Table-10). Thus, the toxicophore analysis highlights genotoxicity, skin sensitisation and environmental toxicity as key structural liabilities, underscoring the need for targeted molecular optimisation and experimental validation to enhance safety and environmental compatibility.

Tox21 pathway: Tox21 pathway profiling of compounds $\mathbf{S_1}$-$\mathbf{S_4}$ revealed consistent activation of nuclear receptor and stress-response pathways. All compounds strongly activated NR-AhR (0.893-0.969) and NR-aromatase (0.792-0.966), indicating xenobiotic sensing and potential disruption of steroid metabolism. Estrogen receptor signaling showed variable but generally moderate to high activation (NR-ER/NR-ER-LBD: 0.552-0.970), while androgen receptor pathways (NR-AR/NR-AR-LBD: 0.655-0.824) were moderately engaged. PPAR-γ activity remained minimal across the series (0.025-0.414) (Table-11). The stress-response pathways were prominently activated, with consistently high SR-ARE (0.822-0.985), SR-MMP (0.713-0.990) and SR-p53 (0.512-0.962) signals, suggesting oxidative stress, mitochondrial dysfunction and cellular stress responses.

Toxicity: *In silico* toxicity profiling revealed a heterogeneous safety landscape across compounds $\mathbf{S_1}$-$\mathbf{S_4}$ (Table-12). All the compounds showed low-to-moderate baseline hERG liability, with increased risk at higher exposure, indicating a manageable cardiotoxic potential. A consistent finding was the high predicted risk of drug-induced liver injury, supported by moderate to high human hepatotoxicity probabilities, identifying hepatic safety as a key concern. Despite generally low AMES mutagenicity and carcinogenicity predictions, uniformly high genotoxicity scores highlight a critical liability requiring experimental validation. Acute oral toxicity was predicted to be low to moderate, suggesting acceptable short-term tolerability. Nephrotoxicity, ototoxicity and hematotoxicity were moderate. Cell-based models indicated low cytotoxicity in RPMI-8226 and A549 cells but higher sensitivity in HEK293 cells.

Radar view: The radar view highlights compound $\mathbf{S_2}$ as the most promising compounds displaying a superior balance across physico-chemical properties, pharmacokinetics and safety parameters compared to compounds $\mathbf{S_3}$, $\mathbf{S_4}$ and the reference compound (Fig. 2).

Boiled egg: The SwissADME Boiled Egg analysis highlights compound $\mathbf{S_2}$ as the most promising candidates with respect to oral bioavailability and BBB permeability, whereas compound $\mathbf{S_4}$ demonstrates acceptable the gastrointestinal absorption without CNS penetration. In contrast, $\mathbf{S_1}$ is positioned near the boundary of the white region, suggesting the moderate absorption with comparatively reduced permeability, likely due to higher TPSA and/or lipophilicity imbalance

TABLE-10
PREDICTED TOXICOPHORE ALERTS AND STRUCTURAL SAFETY ASSESSMENT OF SYNTHESISED COMPOUNDS ($\mathbf{S_1}$-$\mathbf{S_4}$) AND STANDARD DRUG (CICLOPIROX)

Parameter	$\mathbf{S_1}$	$\mathbf{S_2}$	$\mathbf{S_3}$	$\mathbf{S_4}$	Ciclopirox
Aquatic toxicity rule	2	3	3	2	0
Genotoxic carcinogenicity mutagenicity rule	11	1	6	1	2
Nongenotoxic carcinogenicity rule	0	0	1	0	0
Skin sensitisation rule	4	2	4	6	0
Acute toxicity rule	0	0	0	0	0
Nonbiodegradable	3	2	1	1	1
SureChEMBL rule	0	0	0	0	0
FAF-DrugS4 rule	4	2	2	2	0

TABLE-11
PREDICTED Tox21 NUCLEAR RECEPTOR AND STRESS-RESPONSE PATHWAY ACTIVITIES OF SYNTHESISED COMPOUNDS ($\mathbf{S_1}$-$\mathbf{S_4}$) AND STANDARD DRUG (CICLOPIROX)

Parameter	$\mathbf{S_1}$	$\mathbf{S_2}$	$\mathbf{S_3}$	$\mathbf{S_4}$	Ciclopirox
NR-AhR	0.944	0.893	0.956	0.969	0.001
NR-AR	0.368	0.655	0.824	0.737	0.0
NR-AR-LBD	0.431	0.352	0.735	0.334	0.0
NR-Aromatase	0.956	0.966	0.954	0.792	0.970
NR-ER	0.770	0.970	0.823	0.552	0.010
NR-ER-LBD	0.141	0.968	0.148	0.513	0.001
NR-PPAR-gamma	0.025	0.414	0.254	0.117	0.641
SR-ARE	0.822	0.985	0.913	0.965	0.943
SR-ATAD5	0.067	0.677	0.315	0.600	1.000
SR-HSE	0.007	0.495	0.078	0.434	0.998
SR-MMP	0.713	0.990	0.821	0.958	0.418
SR-p53	0.512	0.962	0.811	0.912	0.994

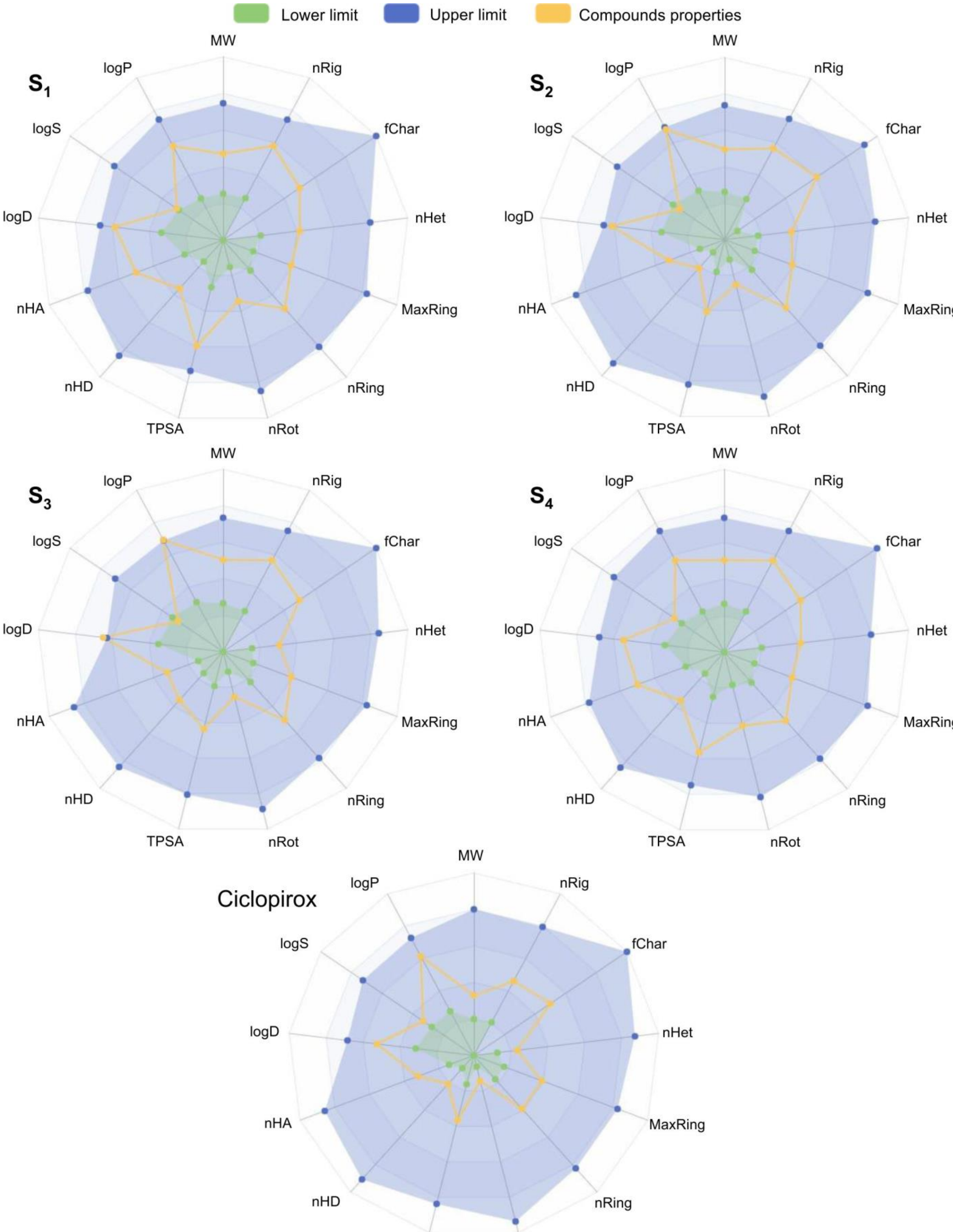

Fig. 2. A radar view detailing for synthesised compounds and standard drug (ciclopirox)

TABLE-12
PREDICTED TOXICITY PROFILES AND ECOTOXICOLOGICAL PARAMETERS OF SYNTHESISED COMPOUNDS (S_1-S_4) AND REFERENCE DRUG (CICLOPIROX)

Parameter	S_1	S_2	S_3	S_4	Ciclopirox
hERG blockers	0.299	0.639	0.301	0.304	0.051
hERG blockers (10 µm)	0.704	0.856	0.730	0.734	0.260
DILI	0.997	0.928	0.954	0.815	0.163
AMES toxicity	0.949	0.141	0.437	0.129	0.344
Rat oral acute toxicity	0.583	0.138	0.520	0.259	0.286
FDAMDD	0.950	0.984	0.975	0.985	0.594
Skin sensitisation	0.989	0.993	0.965	0.885	0.302
Carcinogenicity	0.637	0.196	0.506	0.185	0.302
Eye corrosion	0.0	0.003	0.0	0.0	0.123
Eye irritation	0.701	0.844	0.493	0.207	0.915
Respiratory	0.993	0.994	0.964	0.940	0.742
Human hepatotoxicity	0.708	0.859	0.553	0.666	0.536
Drug-induced nephrotoxicity	0.511	0.967	0.491	0.489	0.295
Drug-induced neurotoxicity	0.962	0.998	0.999	0.992	0.297
Ototoxicity	0.704	0.726	0.671	0.728	0.432
Hematotoxicity	0.841	0.371	0.640	0.628	0.337
Genotoxicity	1.000	1.000	1.000	0.997	0.065
RPMI-8226 immunitoxicity	0.065	0.030	0.053	0.072	0.106
A549 cytotoxicity	0.080	0.022	0.055	0.127	0.102
Hek293 cytotoxicity	0.865	0.980	0.767	0.894	0.315
BCF	1.222	1.829	1.697	0.980	1.684
IGC50	4.107	4.866	4.329	3.642	4.190
LC50DM	4.513	5.630	4.892	4.085	4.861
LC50FM	4.873	6.076	5.403	4.440	5.168

(Fig. 3). These findings are consistent with the predicted ADME profiles and support further biological evaluation of compound S_2 as potential lead compounds.

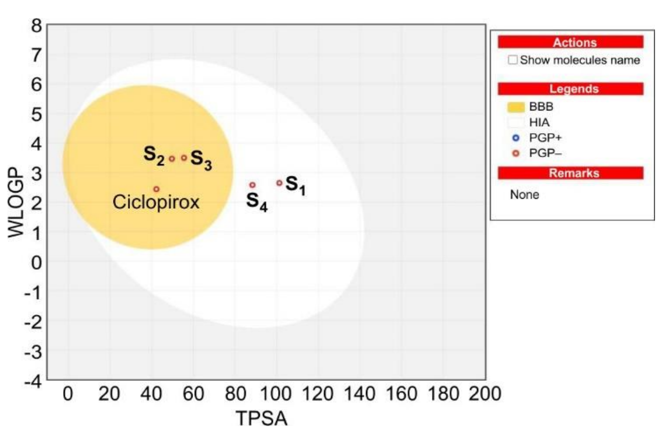

Fig. 3. *In silico* toxicity prediction parameters of synthesised compounds **S1**-S_4 and reference drug (ciclopirox)

Conclusion

The present study successfully established an efficient synthetic strategy for the synthesis of novel 2-methyl-pyridin-3(2*H*)-one derivatives *via* chalcone intermediates and alanine assisted cyclisation. The spectroscopic characterization data confirmed the formation and structural integrity of the synthesised compounds. The *in silico* evaluation demonstrated that the series exhibits favourable drug-like properties, with acceptable physico-chemical parameters and pharmacokinetic behaviour. The molecular docking and PASS predictions indicated promising biological potential, particularly in terms of enzyme inhibition and antimicrobial activity. Among the series, compound S_2 consistently showed superior performance across drug-likeness, docking interactions and ADMET profiles, identifying it as the most promising lead candidate. However, certain limitations were identified, including potential cytochrome P450 inhibition, genotoxicity alerts, and hepatotoxicity risks, which highlight the need for further structural refinement.

CONFLICT OF INTEREST

The authors declare that there is no conflict of interests regarding the publication of this article.

DECLARATION OF AI-ASSISTED TECHNOLOGIES

During the preparation of this manuscript, the authors used an AI-assisted tool(s) to improve the language. The authors reviewed and edited the content and take full responsibility for the published work.

REFERENCES

1. N. Kerru, L. Gummidi, S. Maddila, K.K. Gangu and S.B. Jonnalagadda, *Molecules*, **25**, 1909 (2020); https://doi.org/10.3390/molecules25081909
2. M.M. Heravi and V. Zadsirjan, *RSC Adv.*, **10**, 44247 (2020); https://doi.org/10.1039/D0RA09198G
3. J. Feng, W.-C. Geng, H. Jiang and B. Wu, *Biotechnol. Adv.*, **54**, 107813 (2022); https://doi.org/10.1016/j.biotechadv.2021.107813

4. N.V.S.S. Aishwarya, G.S.P. Matada, R. Pal, I. Aayishamma, K.R. Hosamani, B. Kumaraswamy, B.V. Manjushree and A. Ghara, *J. Mol. Struct*., **1321**, 139655 (2025); https://doi.org/10.1016/j.molstruc.2024.139655
5. M.B. Islam, M.I. Islam, N. Nath, T.B. Emran, M.R. Rahman, R. Sharma and M.M. Matin, *BioMed Res. Int*., **2023**, 9967591 (2023); https://doi.org/10.1155/2023/9967591
6. S. De, S.K. Ashok Kumar, S.K. Shah, S. Kazi, N. Sarkar, S. Banerjee, and S. Dey, *RSC Adv.*, **12**, 15385 (2022); https://doi.org/10.1039/d2ra01571d
7. D.R. Mishra, D.K. Sahoo and N.P. Mishra, *Asian J. Org. Chem.*, **14**, e202500004 (2025); https://doi.org/10.1002/ajoc.202500004
8. Y. Ling, Z.Y. Hao, D. Liang, C.L. Zhang, Y.F. Liu and Y. Wang, *Drug Des. Devel. Ther*., **15**, 4289 (2021); https://doi.org/10.2147/DDDT.S329547
9. G.M. Abu-Taweel, M.M. Ibrahim, H.M. Al-Saidi, M. Alshamrani, S. Khan, F.A. Alhumaydhi and S.S. Alharthi, *Crit. Rev. Anal. Chem*., **54**, 599 (2024); https://doi.org/10.1080/10408347.2022.2089839
10. C. Patel, M. Mohnike, M. C. Hilton and A. McNally, *Org. Lett*., **20**, 2607 (2018); https://doi.org/10.1021/acs.orglett.8b00813
11. T.N. Francisco, N.R. Candeias, S. Guieu, J.L.C. Sousa, R.F.A. Gomes, C.A.M. Afonso, A.M.S. Silva and H.M.T. Albuquerque, *Org. Lett*., **27**, 11757 (2025); https://doi.org/10.1021/acs.orglett.5c03509
12. K.F. Szabó, P. Banachowicz, A. Powała, D. Lunić, I. Funes-Ardoiz, and D. Gryko, *Nat. Commun*., **16**, 5072 (2025); https://doi.org/10.1038/s41467-025-59809-9
13. T.J. Donohoe, S.M. Cooper, R.J.A. Miller and J.R. Bower, *Org. Lett*., **14**, 5400 (2012); https://doi.org/10.1021/ol3024117
14. S.L. Kumar, S. Tabassum, K.S. Sagar and S. Govindaraju, *ChemistrySelect*, **7**, e202203668 (2022); https://doi.org/10.1002/slct.202203668
15. B. Jiang, W.-J. Hao, X. Wang, F. Shi and S.-J. Tu, *J. Comb. Chem*., **11**, 846 (2009); https://doi.org/10.1021/cc900052b
16. T.N. Francisco, H.M.T. Albuquerque and A.M.S. Silva, *Chem. Eur. J.*, **30**, e202401672 (2024); https://doi.org/10.1002/chem.202401672
17. M.A. Elsayed, A.M. Elsayed and F.M. Sroor, *Med. Chem. Res.*, **33**, 476 (2024); https://doi.org/10.1007/s00044-024-03188-1
18. M.B. Islam, M.I. Islam, N. Nath, T.B. Emran, M.R. Rahman, R. Sharma and M.M. Matin, *BioMed Res. Int.*, **1**, 9967591 (2023); https://doi.org/10.1155/2023/9967591
19. P. Shah, *J. Pharm. Res. Int.*, **37**, 97 (2025); https://doi.org/10.9734/jpri/2025/v37i97745
20. A.-L. Villa-Reyna, M. Perez-Velazquez, M.L. González-Félix, J.-C. Gálvez-Ruiz, D.M. Gonzalez-Mosquera, D. Valencia, M.G. Ballesteros-Monreal, M. Aguilar-Martínez and M.-A. Leyva-Peralta, *Int. J. Mol. Sci*., **25**, 7640 (2024); https://doi.org/10.3390/ijms25147640
21. V. Hajhashemi, H. Mojiri-Froshani, L. Saghaei and A. Fassihi, *Adv. Biomed. Res*., **3**, 134 (2014); https://doi.org/10.4103/2277-9175.133276
22. A. Vankar, H. Solanki and A. Ladumor, *Pharma Chem.*, **14**, 7 (2022); https://doi.org/10.4172/0975-413X.14.7.1-9
23. N.B. Patel and S.N. Agravat, *Chem. Heterocycl. Compd.*, **45**, 1343 (2009); https://doi.org/10.1007/s10593-010-0432-2
24. X. Liu, S. Ma, Y. Ding, J. Gao, X. Liu, J. Yao and S. Dai, *Sol. RRL*, **3**, 1800337 (2019); https://doi.org/10.1002/solr.201800337
25. S. Lin, C. Liu, X. Zhao, X. Han, X. Li, Y. Ye and Z. Li, *Front Chem.*, **10**, 869860 (2022); https://doi.org/10.3389/fchem.2022.869860
26. Y. Zhang and A. Pike, *Bioorg. Med. Chem. Lett.*, **38**, 127849 (2021); https://doi.org/10.1016/j.bmcl.2021.127849
27. A. Katrizky, C.A. Ramsden, J.A. Joule and V.V. Zhdankin, Handbook of Heterocyclic Chemistry, edn. 3, pp. 41-42 (2010).
28. A. Rammohan, J.S. Reddy, G. Sravya, C.N. Rao and G.V. Zyryanov, *Zyryanov*, **18**, 433 (2022); https://doi.org/10.1007/s10311-019-00959-w
29. A. Husain, W.A. Ansari, A.R. Khan, M.A. Khan and M. Nasibullah, *Asian J. Chem*., **37**, 3025 (2025); https://doi.org/10.14233/ajchem.2025.34665
30. Y. Ouyang, J. Li, X. Chen, X. Fu, S. Sun and Q. Wu, *Biomolecules*, **11**, 894 (2021); https://doi.org/10.3390/biom11060894
31. C.A. Lipinski, F. Lombardo, B.W. Dominy and P.J. Feeney, *Adv. Drug Deliv. Rev.*, **46**, 3 (2001); https://doi.org/10.1016/s0169-409x(00)00129-0
32. D.F. Veber, S.R. Johnson, H.-Y. Cheng, B.R. Smith, K.W. Ward and K.D. Kopple, *J. Med. Chem.*, **45**, 2615 (2002); https://doi.org/10.1021/jm020017n
33. T. Sander, OSIRIS Property Explorer (2001).
34. A.A. Lagunin, A.V. Stepanchikova, D.A. Filimonov and V.V. Poroikov, *Bioinformatics*, **16**, 747 (2000); https://doi.org/10.1093/bioinformatics/16.8.747
35. D.S. Goodsell and A.J. Olson, *Proteins*, **8**, 195 (1990); https://doi.org/10.1002/prot.340080302
36. G.M. Morris, R. Huey, W. Lindstrom, M.F. Sanner, R.K. Belew, D.S. Goodsell and A.J. Olson, *J. Comput. Chem*., **30**, 2785 (2009); https://doi.org/10.1002/jcc.21256
37. A. Daina, O. Michielin and V. Zoete, *Sci. Rep*., **7**, 42717 (2017); https://doi.org/10.1038/srep42717
38. D.E.V. Pires, T.L. Blundell and D.B. Ascher, *J. Med. Chem*., **58**, 4066 (2015); https://doi.org/10.1021/acs.jmedchem.5b00104
39. F. Cheng, W. Li, Y. Zhou, J. Shen, Z. Wu, G. Liu, P.W. Lee and Y. Tang, *J. Chem. Inf. Model*., **59**, 3667 (2019); https://doi.org/10.1021/acs.jcim.9b00969
40. P. Banerjee, A.O. Eckert, A.K. Schrey and R. Preissner, *Nucleic Acids Res*., **46**, W257 (2018); https://doi.org/10.1093/nar/gky318
41. R. Huang, M. Xia, D. Sakamuru, J. Zhao, S. Shahane, A. Attene-Ramos, A. Simeonov and R.S. Judson, *Front. Environ. Sci*., **3**, 85 (2016); https://doi.org/10.3389/fenvs.2015.00085